



Rapid Manufacturing of Co-Cr-Mo Implants by Three-Dimensional Printing Process for Orthopedic Applications

Mahdi Dourandish^a, Abdolreza Simchi^{a,b,*}, Dirk Godlinski^c

^aDepartment of Material Science and Engineering,

^bInstitute for Nanoscience and Nanotechnology, Sharif University of Technology, Tehran, Iran,

^cFraunhofer Institute for Manufacturing Technology and Applied Materials Research IFAM, Wiener, Germany

Abstract

The fabrication of complex-shaped parts out of (wt %) Co-28Cr-6Mo alloy by three-dimensional printing (3DP) was studied using two grades of the alloy with average particle sizes of 20 and 75 μm . To produce sound specimens, 3DP processing parameters were tuned. The sintering behavior of the powders was characterized by the dilatometric analysis. Batch sintering in argon atmosphere at 1280 °C for 2h was also performed. It was shown that complex-shaped biomedical parts with total porosity of 12-25% and homogenous pore structure can be fabricated by the 3DP process.

Keywords: Biomaterial; Co-Cr-Mo alloy; Rapid manufacturing; Three dimensional printing.

Received: December 1, 2007; **Accepted:** February 5, 2008

1. Introduction

Rapid prototyping technologies can create physical parts directly from CAD models by generating a number of layers of a given material [1]. One of the most flexible processes is three-dimensional printing (3DP) [2]. In this process, a polymeric binder is used as glue to bound powder particles together layer by layer. Figure 1 shows a schematic sequence of the process. Green parts of arbitrary forms with complex-shapes can be fabricated by CAD models. Since the part is fully supported by unbound, underlying powder, large

overhangs, undercuts and complex internal geometries could be produced [4]. Providing a tremendous flexibility of part geometry that 3DP can fabricate, this technology creates a great interest in manufacturing biomaterial parts such as implants and instruments.

This paper deals with 3DP of Co-Cr-Mo alloy. The cobalt based alloy containing 28% chromium and 6% molybdenum has applications in fabrication of medical implants [5]. These alloys demonstrate the most useful balance in strength, fatigue and wear [6, 7] along with resistance to corrosion [8-10]. Although fabrication of surgical implants by conventional methods, *i.e.* casting and metal forming, are common it is of interest to fabricate implants directly from powder particles using CAD data. This would increase

*Corresponding author: Abdolreza Simchi, Institute for Nanoscience and Nanotechnology, Sharif University of Technology, P.O.Box: 11365-9466, Azadi Avenue, 14588, Tehran, Iran.
Tel. and Fax: (+98)21-6616 5261
E-mail: simchi@sharif.edu

the flexibility of designing implants and speed up the production route. In this paper, the viability of the 3DP in rapid manufacturing of implants with complex-shaped is shown.

2. Materials and methods

2.1. Materials

Co-28Cr-6Mo (nominal composition in wt%) gas atomized powders with two different average particle sizes of 20 and 75 μm were used in the present study. The finer Co-Cr-Mo alloy was supplied by Sirona GmbH (Germany) while the coarser one was purchased from Osprey Ltd. (UK). Figure 2 shows SEM micrograph of the powder particles, exhibiting nearly spherical grains with a broad size distribution. Figure 3 shows the differential scanning calorimetry (DSC) curves of the powders. A liquid phase is formed at 1266 and 1279 $^{\circ}\text{C}$ for the fine (F) and coarse (C) powders, respectively. The slight difference in the solidus temperature can be related to the particle size effect as well as the difference in the carbon content (about 0.08% wt).

2.2. 3D Printing and sintering

Small cylindrical test specimens (15 mm diameter and 10 mm height) were fabricated by a commercially available 3D-printer machine (RX-1, Prometal, USA). A standard

water-based binder (PM-B-SR2-02) was provided by Prometal Co, USA. The studied processing parameters included: a) the drying time of a printed layer; b) the speed of powder spreading; c) the layer thickness. After building sound test parts, the specimens were dried in a small oven at 230 $^{\circ}\text{C}$ for 60 min. in air and sintered at 1280 $^{\circ}\text{C}$ in argon atmosphere. The heating and cooling ramps were 5 and 10 $^{\circ}\text{C}/\text{min.}$, respectively. In order to determine the sintering response of the powder materials, a sinter dilatometer (TMA 801, Bahr, Germany) was used.

2.3. Characterization

The density of the sintered specimens was determined by the water displacement method (Archimedes' method). Microstructural study was performed on the cross-sections of the sintered parts perpendicular to the printing direction. The amount of carbon pick up upon de-binding and sintering was analyzed by a LECO Carbon Analyzer.

3. Results and discussion

3.1. Sintering of loose powders

Figure 4 shows the dilatometric curves of the examined powders. As seen, the sintering response is influenced by the powder particle size. In the case of fine powder, the shrinkage starts at ~ 1000 $^{\circ}\text{C}$ and the maximum

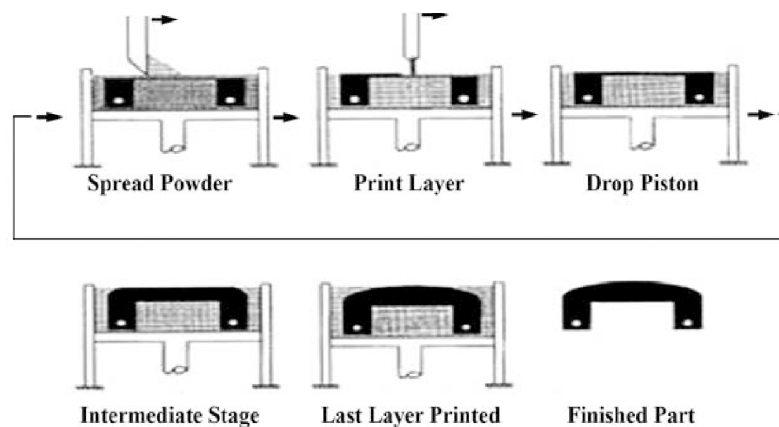


Figure 1. The process sequences of three dimensional printing [3].

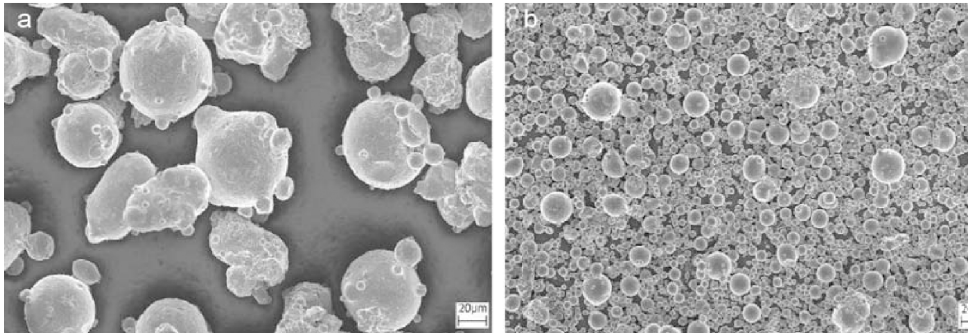


Figure 2. SEM micrographs of Cr-Co-Mo coarse (a) and fine (b) powders.

shrinkage rate occurs at 1269 °C. According to the DSC curve (Figure 3), the solidus temperature of the alloy is 1266 °C. Therefore, at the higher temperatures the materials turns mushy and rapid densification is attained by particles rearrangement and grain shape accommodation. The coarse powder exhibited maximum shrinkage rate at much higher temperature of 1280 °C due to lower surface area of the particles. Apparently, liquid phase sintering must be used in order to achieve a high densification rate during heating up.

3.2. 3D Printing

Table 1 shows the results of many tests performed to find proper 3DP processing parameters. It was found that at a constant binder amount per area, the layer thickness is

the most important factor affecting the soundness of the printed parts. Using a high layer thickness leads to unbounded layers whilst a low layer thickness results in pushing away of the printed layers during spreading of the next powder layer. The proper layer thickness was determined to be 75 and 150 μm for the fine and coarse powders, respectively. On the other hand, the duration time for the curing of the binder should be high enough to achieve sufficient green strength. It was found that 60 s with a powder spreading speed of 10 mm/s yield reasonable result.

Figure 5a shows the green density of the 3D printed cylinders produced at the optimum condition. The tap density of the powders is included for comparison. The green density

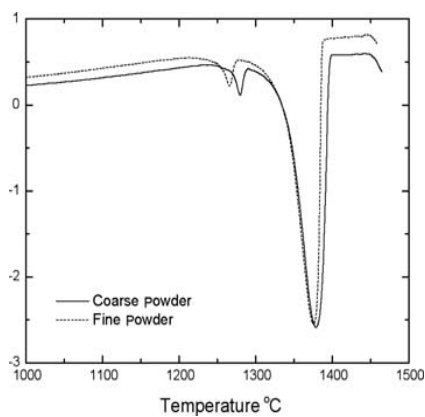


Figure 3. DSC curves of the examined powders.

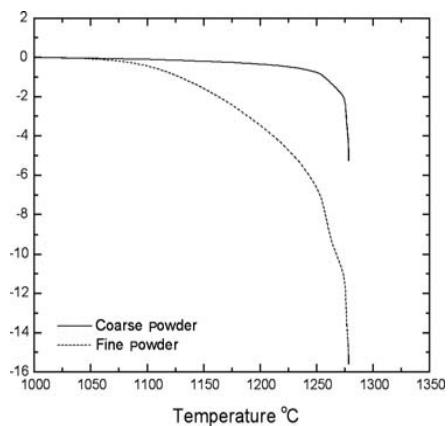


Figure 4. Dilatometric curves of Co-Cr-Mo powders sintered at 1280 °C for 120 min. in argon atmosphere.

Table 1. Effect of 3DP processing conditions on the quality of the printed parts.

No.	Drying time (s)	Spreading speed (mm/s)	Layer thickness (μm)	Observations	
				Fine powder	Coarse powder
1	30	30	75	PL, AP	-
2	30	30	100	UL, PL, AP	PL
3	30	30	150	-	PL
4	30	10	75	AP	-
5	30	10	100	UL, PL, AP	PL
6	30	10	150	-	Fine PL
7	60	30	75	AP	-
8	60	30	100	UL, AP	PL
9	60	30	150	-	Fine PL
10	60	10	75	Best of all	-
11	60	10	100	UL	PL
12	60	10	150	-	Best of all

PL: pushed layers; AP: agglomerated particles; UL: unbound layers.

of the printed coarse powders is nearly equal to the tap density whilst the fine powders yielded lower density. This suggests that during 3D printing, agglomeration of the fine particles is likely to occur. As it will be shown in the next section, the agglomeration of powder particles influences the densification of the green part during sintering.

3.3. Sintering

Figure 5b shows the density of the specimens sintered at 1280 °C for 120 min. The density of the gravity-sintered powders is included in the graph for comparison. One can notice the higher densification of 3DP parts compared with the tapped powders when the coarse particles were used. This is in contrast with what is seen for the fine

particles. This observation indicates that, the agglomerated particles caused a network of large pores, could be removed during sintering.

3.4. Microstructure

Figure 6 shows the cross-sections of the sintered 3DP parts. One can notice the large pores in the microstructure of the part produced from 20 μm Co-Cr-Mo powder (Figure 6a). Many small pores are also visible. In contrast, the microstructure of parts made from the coarse powder (Figure 6b) consists of relatively homogenous large pores that can be suitable for biomedical application. Since, the carbon content of the alloy is crucial for corrosion resistance, carbon pick up during de-binding and sintering was analyzed. The

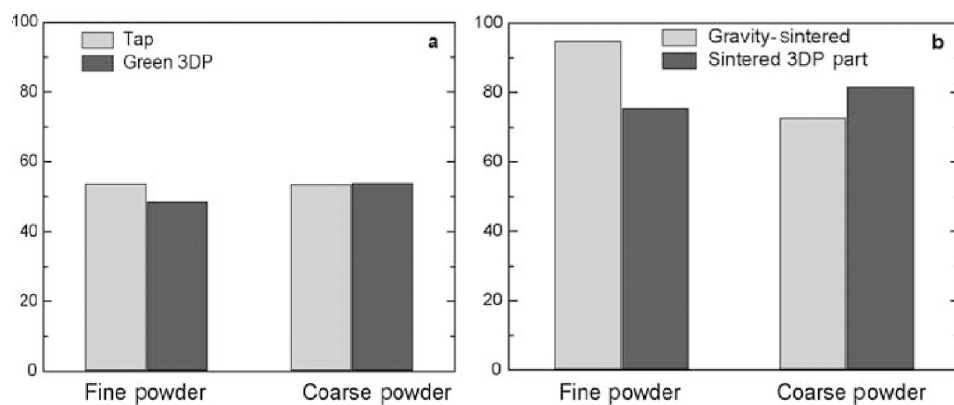


Figure 5. Green density of 3DP cylinders compared with tap density of raw powders (a) and effect of sintering on the densification of 3DP parts and gravity-sintered powders (b).

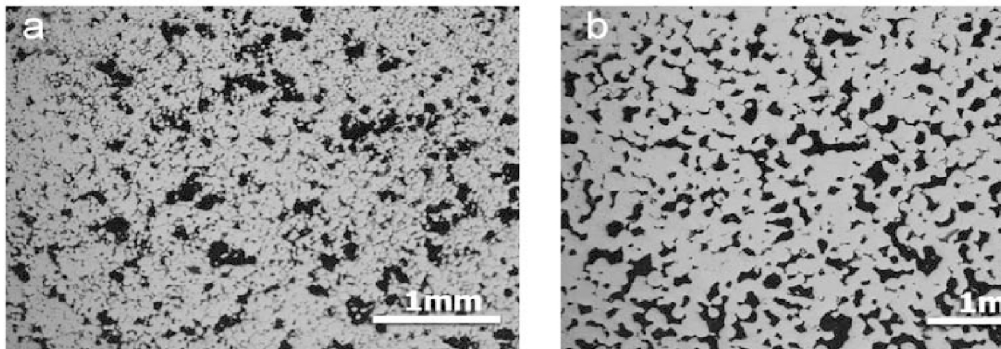


Figure 6. Cross-sections of printed parts out of fine (a) and coarse (b) powders after sintering at 1280 °C for 120 min.

results of carbon measurements showed that the amount of carbon pick up is 0.2 and 0.07 wt% for the fine and coarse powders, respectively. This is attributed to the lower layer thickness used for 3DP of the fine powders, which directly influences the amount of binder used for printing. Additionally, the debinding of green parts composed of finer particles needs more attention since the pore channels are smaller.

When the optimum condition of processing has been determined, a case study was performed to show the viability of the procedure. Figure 7 shows a picture of a small femoral stem model produced by 3DP from Co-Cr-Mo powder. The density of the part is 80% theoretical. The part is sound without any cracks or warpage. Hence, it has become clear that the 3DP process can be used to fabricate complex-shaped implants directly from CAD data. Nevertheless, further work is required to measure the mechanical strength of the sintered specimens, particularly the

figure behavior, in order to access the suitability of the technique.

4. Conclusion

3DP process was used to fabricate biocompatible components out of Co-28Cr-6Mo (wt%) powders. It was shown that powders with average particle size of 75 μm can be used for successful manufacturing of complex-shaped parts. The layer thickness of 150 μm , spreading speed of 10 mm/s, and drying time of 60 s should be used for the printing process. Sintering at 1280°C for 120 min. yields sound parts with ~20% porosity. The pores are open and large to get tissue the possibility of in growth. Lower sintering temperatures are also usable because initial sintered contacts starts at relatively low temperature of 1000°C. The amount of porosity can be tailored dependent on the application.

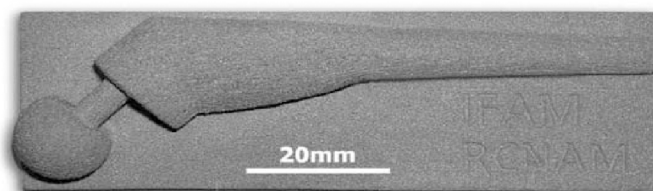


Figure 7. A prototype of Co-Cr-Mo femoral stem produced by 3DP process.

5. References

- [1] Simchi A, Petzoldt F, Pohl H. On the development of direct metal laser sintering for rapid tooling. *Mater Proces Tech* 2003; 141: 319-28.
- [2] Godlinski D, Pohl H, Morvan S. Rapid manufacturing of dense stainless steel parts by 3D Printing. *Euro PM* 2004; 2: 131-6.
- [3] <http://www.compositesiq.com>. Accessed in June 2007.
- [4] Liu J, Kuhn H, Rynerson M, Morvan S. Binder technology for large metal parts produced using three-dimensional printing. *Euro PM*; 5: 153-7.
- [5] Moraux JY, Pierronnet M. PM used for bio-metallic materials application to a cobalt base alloy with 28% Cr and 6% Mo. *Euro PM*; 4: 845-51.
- [6] Katti KS. Biomaterials in total joint replacement. *Colloid Surfac B* 2004; 39: 133-42.
- [7] Hsu HC, Lian SS. Wear properties of Co-Cr-Mo-N plasma-melted surgical implant alloys. *Mater Proces Tech* 2003; 138: 231-5.
- [8] Okazakia Y, Gotoh E. Comparison of metal release from various metallic biomaterials *in vitro*. *Biomaterials* 2005; 26:11-21.
- [9] Lin HY, Bumgardner JD. *In vitro* biocorrosion of Co-Cr-Mo implant alloy by macrophage cells. *Orthopaedic Res* 2004; 22: 1231-6.
- [10] Hsua RW, Yang CC, Huangc CA, Chenb YS. Electrochemical corrosion studies on Co-Cr-Mo implant alloy in biological solutions. *Mater Chem Phys* 2005; 93: 531-8.
- [11] Krasicka-Cydzik E, Oksiuta Z, Dabrowski JR. Corrosion testing of sintered samples made of the Co-Cr-Mo alloy for surgical applications. *Mater Sci* 2005; 16: 197-202.
- [12] Bhat SV. *Biomaterials*. Alpha Science International Ltd. 2005; pp. 118-55.

